Void growth in power-law creeping solids: Effect of surface diffusion and surface energy

ARTICLE *in* INTERNATIONAL JOURNAL OF SOLIDS AND STRUCTURES · DECEMBER 2005

Impact Factor: 2.21 · DOI: 10.1016/j.ijsolstr.2005.06.048

3 AUTHORS, INCLUDING:

Sankara J. Subramanian
Indian Institute of Technology Madras
13 PUBLICATIONS **32** CITATIONS

SEE PROFILE

Pedro Ponte Castañeda
University of Pennsylvania
169 PUBLICATIONS **4,552** CITATIONS

SEE PROFILE

Available online at www.sciencedirect.com
SCIENCE DIRECT®
ELSEVIER
International Journal of Solids and Structures 42 (2005) 6202–6225
INTERNATIONAL JOURNAL OF SOLIDS and STRUCTURES
www.elsevier.com/locate/ijsolstr

Void growth in power-law creeping solids: Effect of surface diffusion and surface energy

S.J. Subramanian [a], P. Sofronis [b,*], P. Ponte Castaneda [c]

[a] *Intel Corporation, Mailstop CH5-157, 5000 W. Chandler Blvd., Chandler, AZ 85226, USA*
[b] *University of Illinois at Urbana-Champaign, Department of Mechanical and Industrial Engineering, 158 Mechanical Engineering Building, 1206 West Green Street, Urbana IL 61801, USA*
[c] *University of Pennsylvania, Department of Mechanical Engineering and Applied Mechanics, 297 Towne Building, 220 S. 33rd Street, Philadelphia, PA 19104, USA*

Received 16 May 2004; received in revised form 8 June 2005

Abstract

This paper addresses the growth of a void in a nonlinearly creeping material in the presence of the void-surface energy effect and void-surface diffusion driven by surface curvature gradients. Large strain finite element analysis of the coupled problem indicates that microstructural variables (porosity and void aspect ratio), as well as macroscopic deformation rates are strongly affected by the relative strength of the void-surface energy effect and the void-surface diffusion process vis-a-vis the rate of creep deformation in the bulk of the solid. The phenomenon is characterized by two-dimensionless groups, one measuring the strength of the surface diffusion process with respect to the nonlinear creep deformation in the interior of the solid, and the other the magnitude of the surface energy of the void in relation to the applied load and the size of the void. The computations reveal a rich variety of solutions that reflect a wide range of external load, material, and geometric parameters. Classical void growth studies that ignore both surface diffusion and surface energy effects are shown to recover only one case of this family of solutions. The computations also serve to quantitatively evaluate recent constitutive theories for porous nonlinear materials that account for continuously evolving microstructure, but do not include surface diffusion or surface energy effects.

Keywords: Material creep behavior; Porous media; Voids; Surface diffusion; Surface energy

* Corresponding author. Fax: +1 217 244 6534.
E-mail address: sofronis@uiuc.edu (P. Sofronis).

0020-7683/$ - see front matter © 2005 Elsevier Ltd. All rights reserved.
doi:10.1016/j.ijsolstr.2005.06.048

1. Introduction

It is well-known that the growth of small voids in inelastic materials plays a central role both in ductile fracture of metals at room temperature and creep rupture at elevated temperatures. Previous investigations have dealt with void growth in both nonlinearly viscous solids (e.g., Budiansky et al., 1982; Needleman et al., 1995) and materials deforming by rate-independent plasticity (e.g., see the reviews of Tvergaard, 1989; Needleman et al., 1992). The present investigation focuses on void growth in nonlinearly viscous solids, specifically of the power-law creeping type. For these materials, the work done to date has addressed the evolution of the shape and size of voids with time. Budiansky et al. (1982) have obtained detailed solutions for a void growing in an infinite viscous matrix under a variety of remote axisymmetric loading states. More recently, Needleman et al. (1995) have considered the effect of void interaction and void shape change on the void growth rates through extensive finite-element calculations, also under axisymmetric conditions. The cell model employed by them is that of Needleman and Rice (1980) who studied growth of cavities occurring by the combined action of grain-boundary diffusion and power-law creep in the adjoining grains. Their analysis was employed by Sham and Needleman (1983) to study the effect of triaxial stressing on diffusive cavity growth.

Although it is well understood that mass transfer over the void-surfaces is of great relevance in determining surface profiles, and indeed demonstrated through numerical computations (Subramanian and Sofronis, 2001, 2002), in the studies to date on void growth, very little attention has been paid to the process of surface diffusion over the void-surfaces. In the classical void growth models (e.g., Budiansky et al., 1982; Needleman et al., 1995), the void shapes are affected only by the viscous deformation of the solid; reconfiguration of the void-surface due to mass transport over it due to surface diffusion is completely ignored. On the other hand, in the creep cavitation models (e.g., Needleman and Rice, 1980; Sham and Needleman, 1983), surface diffusion is assumed to be extremely fast leading to a void that always maintains a spherical-caps shape. Chuang et al. (1979) developed models for diffusive cavitation that were not based on a quasi-equilibrium void shape, and allowed the void shape to be determined as part of the solution; however, the grains were assumed to be rigid. Thus, none of these models account for void shapes that result from the concurrent action of void-surface diffusion and nonlinear bulk deformation. A notable exception to this is the work of Suo and Wang (1994) and Wang and Suo (1997) who studied the interaction of void-surface diffusion with the elastic deformation in the surrounding matrix under biaxial tension. These investigators found that when the void-surface energy effect is dominant the void evolves to an equilibrium shape close to an ellipse, whereas when the bulk elastic energy effect dominates the void never reaches equilibrium and crack-like shape instabilities emerge. It should be noted though that the classical Laplace relationship between the void curvature, void-surface energy, and the normal traction in the adjoining bulk material (Herring, 1951; Rice and Chuang, 1981) was not enforced in any of these calculations.

Based on these results and those of Subramanian and Sofronis (2001, 2002), one concludes that the interaction between void-surface diffusion and bulk deformation mechanisms plays a vital role in determining the void shape and size changes. Further, as length scales relevant to modern engineering applications shift from microns to nanometers, surface energy effects and hence the void-surface traction take on increased significance. For instance, in a material with a surface energy γ_p of 1 J/m^2 (a typical value for metals), normal tractions in the bulk material adjoining a void of radius 1nm are of the order of 1 GPa. Certainly, no claim is being made here that the present continuum mechanics study will be applicable at the level of clusters of atoms. However, it is emphasized that that surface energy effects will be more prominent as void size decreases from tens of microns to hundreds of nanometers.

On the other hand, rigorous constitutive theories for the macroscopic response of nonlinearly deforming voided materials in the absence of any void-surface diffusion or surface energy effects have been proposed by Ponte Castañeda and coworkers (Ponte Castañeda and Zaidman, 1994; Kailasam and Ponte Castañeda, 1996; Ponte Castañeda, 1997; Kailasam et al., 2000). Apart from a relationship between the overall

deformation rate of the solid and the applied loads, these constitutive theories also report evolution equations for the microscopic variables, such as porosity, void aspect ratio, and void orientation. It should be noted that the constitutive descriptions of these works are derived from variational approximations, and that their accuracy has not been evaluated in detail using numerical computations. It should also be noted that an alternative approach—one that has the advantage of reducing to the Gurson model for high triaxiality, but which is less general, allowing only the development of transversely isotropic symmetries—has been proposed by Golaganu et al. (1993, 1994).

For a void subjected to remote uniaxial tension, the bulk creep deformation tends to elongate an initially circular void (Budiansky et al., 1982), whereas the surface diffusion process over the void-surface acts to maintain the circular shape. Further, void-surface energy considerations dictate that part of the work rate delivered by the external loads in deforming the solid be expended on changing the size of the void (Subramanian and Sofronis, 2001). In the present work, this competition between nonlinear creep deformation in the bulk and void-surface diffusion during void growth is addressed in the presence of void-surface energy effects. The normal tractions on the void-surface induced by the curvature of the void are accounted for in the formulation of the relevant problem. As first derived elsewhere (Subramanian and Sofronis, 2001, 2002), the surface diffusion process and the void-surface energy effect are characterized by dimensionless groups that measure their relative strengths with respect to the power-law creep process in the surrounding matrix and the applied loads. The numerical computations which are performed using a large-strain formalism (Subramanian, 2001) are grouped in two sets: the first deals with the effect of creep nonlinearity and porosity on the macroscopic deformation and void growth in the absence of void-surface diffusion and energy effects, while the second elaborates on the effect of the surface diffusion and surface energy. The computations yield the overall macroscopic deformation rates, as well as details of the evolution of void size and shape, all of which are used for quantitative comparisons with the constitutive theories of Ponte Castañeda and co-workers. All computations are performed on a unit cell with the deformation occurring under plane strain conditions, and in both sets of studies, results are presented for different initial unit cell porosities. A question that arises here is whether the present computation results which are conducted for cylindrical voids arranged in a rectangular array are still valid for spherical voids arranged in a rectangular array. Certainly, the deformation mechanisms that will be active will be identical in the two cases. The surface diffusion process will be dependent on two principal curvatures in the three-dimensional case, and the complexity of possible pore shapes is far greater in the three-dimensional case compared to the two-dimensional case. However, the trends reported in this study should still hold in the three-dimensional case, because the underlying deformation processes remain the same: The applied loads tend the distort the solid and the void; the surface diffusion process tries to maintain the spherical shape of the void, whereas the strength of the surface energy will dictate the energy expenditure to cause changes in void shape.

2. Material constitutive laws

The bulk material of the porous solid is incompressible, and undergoes finite deformation by power-law creep governed by the constitutive equation:

$$\mathbf{D} = 3C\sigma_{\mathrm{e}}^{n-1}\mathbf{s}/2, \tag{1}$$

where $\mathbf{D}$ is the rate of deformation tensor (the symmetric part of the velocity gradient), $\mathbf{s}$ is the deviatoric part of the Cauchy stress $\boldsymbol{\sigma}$, $\sigma_{\mathrm{e}} = \sqrt{3\mathbf{s}:\mathbf{s}/2}$ is the equivalent stress, n is the creep exponent, and $C \equiv \dot{\varepsilon}_0/\sigma_0^n$ is the creep modulus with $\dot{\varepsilon}_0$ and σ_0 being material parameters in the uniaxial tension relation $\dot{\varepsilon}/\dot{\varepsilon}_0 = (\sigma/\sigma_0)^n$. Diffusion along the void-surface is driven by chemical potential gradients (Herring, 1951) such that

$$j_{\mathrm{p}} = \mathscr{D}_{\mathrm{p}}\mathrm{d}(\gamma_{\mathrm{p}}k)/\mathrm{d}s, \tag{2}$$

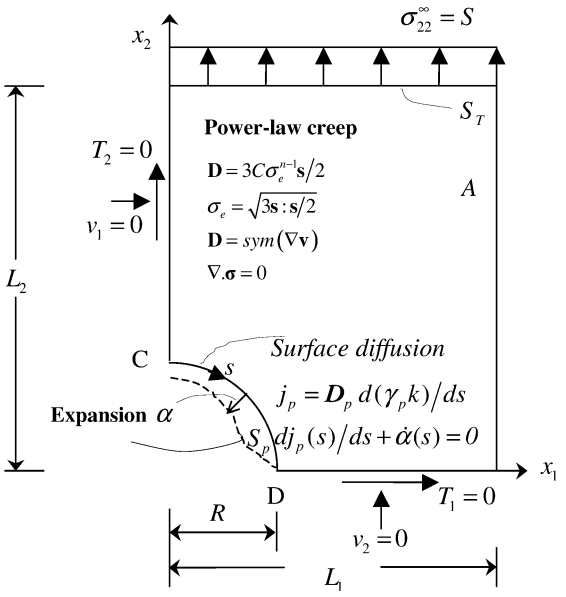

Fig. 1. Description of the initial/boundary-value problem.

where j_{p} is the volumetric flux per unit length along the void surface, $\mathscr{D}_{\mathrm{p}} = D_{\mathrm{p}}\delta_{\mathrm{p}}\Omega/KT$ is the void-surface diffusivity having dimensions of volume divided by stress per unit time, D_{p} is the diffusion coefficient, δ_b is an effective thicknesses through which matter diffuses, k and γ_{p} are respectively the curvature and the energy of the void-surface, Ω is the atomic volume of the diffusing species, K is Boltzmann's constant, T is the absolute temperature, and s is arc length along the void-surface (Fig. 1). Along the void-surface, matter conservation dictates that

$$\frac{\mathrm{d}j_{\mathrm{p}}(s)}{\mathrm{d}s} + \dot{\alpha}(s) = 0, \tag{3}$$

where $\dot{\alpha}(s)$ is the local void-surface expansion rate (Fig. 1) measured normal to the void-surface and is positive when matter is deposited on the void-surface and negative when the void-surface is eroded. Here it should be emphasized that $\dot{\alpha}$ is not the velocity of any material point on the void-surface; it is simply the rate at which mass is added to or removed from the void-surface.

Equilibrium at any arbitrary point on the void-surface is described by the standard Laplace equation (Gurtin and Murdoch, 1975; Rice and Chuang, 1981; Freund et al., 1993) that relates the normal traction σ_{n} from the adjoining bulk material to the local curvature k

$$\sigma_{\mathrm{n}}(s) = \gamma_{\mathrm{p}} k(s). \tag{4}$$

In the present model, the surface tension γ_{p} is assumed to be constant and therefore, the tangential stress on the void-surface is zero (Rice and Chuang, 1981; Freund et al., 1993). A void that is concave when seen from the bulk has positive curvature, and leads to tensile stresses in the adjoining bulk material.

3. The unit cell model

Void growth in a porous creeping solid is investigated under plane strain conditions by assuming cylindrical voids arranged in a rectangular array. Owing to the symmetry in the deformation under tensile

loading, the first quadrant of a unit cell containing a void was analyzed (see Fig. 1). At time $t = 0$, the void is circular of radius R, and the initial unit cell is a rectangle of dimensions $L_1 \times L_2$. Thus, the initial porosity of the unit cell is $f_0 = \pi R^2/4L_1L_2$ and the initial void aspect ratio $w_0 = a_2/a_1 = 1$. In general, as the solid deforms, the void changes shape and size, and its axes a_1 and a_2 vary with time. The symmetric arrangement of the voids is maintained throughout the course of deformation of the solid under remotely applied stresses $\sigma^{\infty}_{11} = \sigma^{\infty}_{12} = 0$, and $\sigma^{\infty}_{22} = S$. Standard symmetry conditions were enforced on the axes of symmetry $x_1 = 0$ and $x_2 = 0$. The top face normal to the direction of stressing was required to remain horizontal during deformation and free of shear traction. The right face was constrained to remain vertical with zero shear stress and zero average normal stress. In all the results presented in this paper, S is positive.

The solution to the deformation of the voided material is obtained in time incrementally and the relevant initial/boundary-value problem is set up as shown in Fig. 1. At every time step, the solutions process addresses the deformation of the bulk material and the change of the void-surface due to surface diffusion. The solution procedure involves the solution of three coupled problems in succession (Subramanian, 2001): In problem (i) the solution to the displacement increments over a time increment is obtained by solving for the bulk deformation of the unit cell under the externally applied tractions (load) and the void-surface tractions induced by the void-surface curvature. The solution to this problem enforces equilibrium in the bulk of the matrix and ensures the satisfaction of Laplace relation (4) on the void-surface. The configuration of the void-surface as obtained from the solution to problem (i) forms the basis for the solution to problem (ii), wherein one solves for expansion increments over the void-surface due to mass removal or deposition subject to the conditions that mass flux vanishes at points C and D (Fig. 1) owing to the symmetry of the void arrangement and loading. Solution to problem (ii) ensures mass conservation on the void-

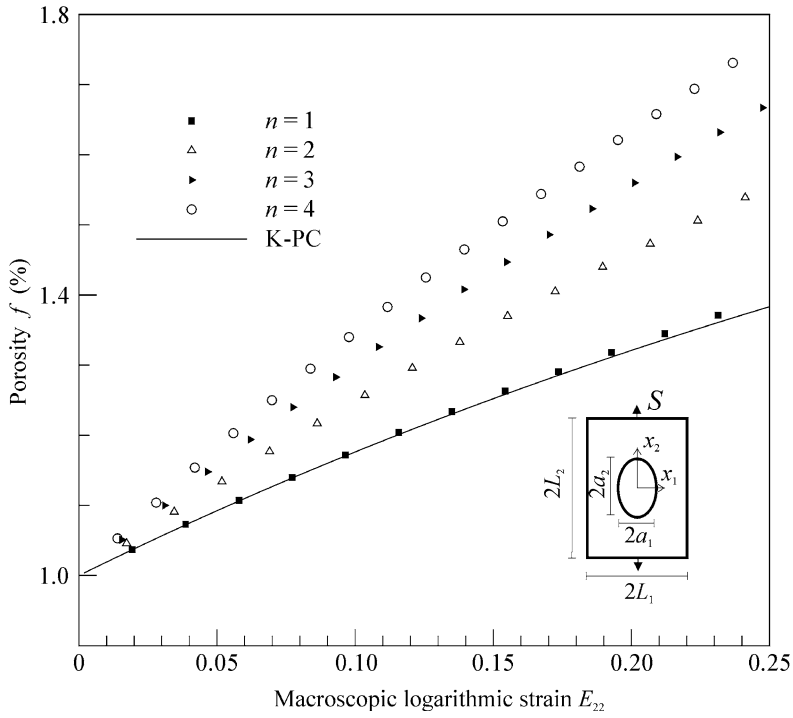

Fig. 2. Evolution of porosity as a function of the creep exponent n: $f_0 = 0.01$, $L_p/R = 0.01$, and $\psi_p = 5 \times 10^{-8}$ (no diffusion or surface energy effects). All symbols denote results from the finite-element computations of the present work, and "K–PC" refers to the results obtained using the theory of Kailasam and Ponte Castañeda (1996).

surface as dictated by Eq. (3), as well as enforcement of the void surface diffusion Eq. (2). In problem (iii) the bulk deformation problem is re-solved by calculating corrections to the displacement increments obtained in problem (i) under applied displacement increments on the void-surface equal to the expansion increments of the void surface obtained from the solution to problem (ii). Effectively, in problem (iii) the solution to the matrix bulk deformation (displacement increments) and stresses as obtained in problem (i) is modified in order for the incremental expansion of the void-surface due to void-surface diffusion over the time increment to be accounted for. It should be emphasized that the three-step scheme outlined above is an approximate one; in principle, one should perform successive bulk deformation and surface expansion corrections until converged bulk displacement increments as well as surface expansion increments are obtained for the time increment. However, since such a convergence study was not included in the present study, care was taken to take appropriately small time increments so that the three-step iterative scheme would still be accurate.

An updated Lagrangian formulation is employed wherein the configuration of the unit cell obtained by updating the nodal coordinates with the displacement increments computed from the iterative numerical scheme is taken to be the instantaneous reference configuration. In this formulation, the matrix $\mathbf{N}_{\mathrm{L}}$ relates the velocity $\mathbf{v}$ to the velocities at the nodes of a mesh representing the current, deformed geometry (analogous to the matrix $\mathbf{N}$, which relates the velocity $\mathbf{v}$ to the nodal velocities of an undeformed mesh in a small-strain formulation). In finite-element notation, the vectors for the velocity $\mathbf{v}$ and the velocity gradient $\mathbf{L} = \partial\mathbf{v}/\partial\mathbf{x}$ are written in terms of the nodal velocities as

$$\mathbf{v} = \mathbf{N}_{\mathrm{L}}\mathbf{v}^{N}, \quad \text{and} \quad \mathbf{L} = \mathbf{B}_{\mathrm{L}}\mathbf{v}^{N}, \tag{5}$$

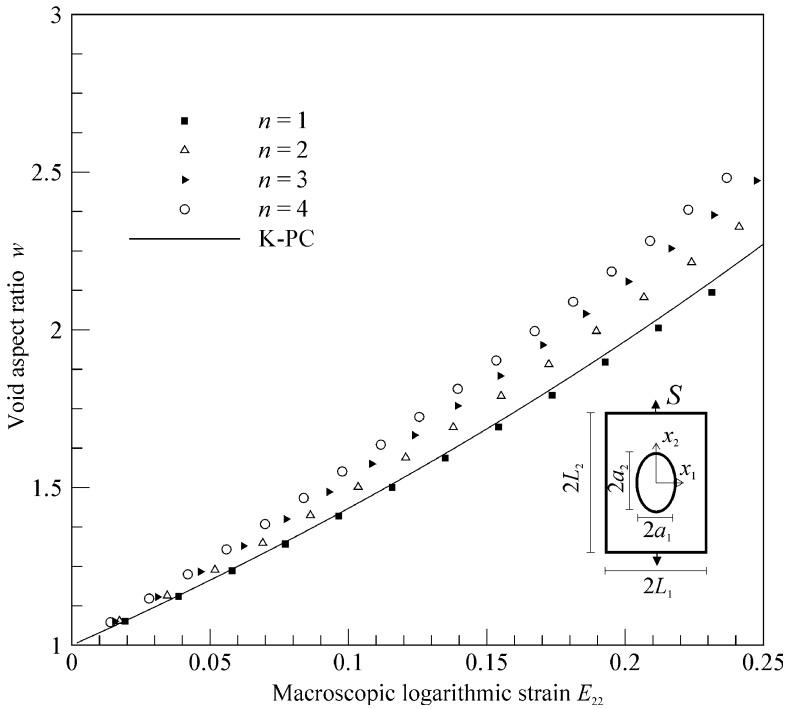

Fig. 3. Evolution of void aspect ratio $w = a_2/a_1$ as a function of the creep exponent n: $f_0 = 0.01$, $L_{\mathrm{p}}/R = 0.01$, and $\psi_{\mathrm{p}} = 5 \times 10^{-8}$ (no diffusion or surface energy effects). All symbols denote results from the finite-element computations of the present work, and "K–PC" refers to the results obtained using the theory of Kailasam and Ponte Castañeda (1996).

where $\mathbf{B}_{\mathrm{L}}$ is the matrix of spatial derivatives of the matrix $\mathbf{N}_{\mathrm{L}}$, the subscript L denotes large deformation, and the matrices $\mathbf{N}_{\mathrm{L}}$ and $\mathbf{B}_{\mathrm{L}}$ depend on the deformed mesh coordinates.

In order to solve the bulk deformation problem (problem (i)), one starts with the principle of virtual power for the unit cell, which in the present case after incorporating Eq. (4) is stated as

$$\int_{S_T} T_i v_i^* \,\mathrm{d}s = \int_A \sigma_{ki} \frac{\partial v_i^*}{\partial x_k} \,\mathrm{d}A + \int_{S_\mathrm{p}} \gamma_\mathrm{p} k v_n^* \,\mathrm{d}s. \tag{6}$$

Here T_i is specified traction on the external boundary S_T (i.e. $x_2 = L_2$ in Fig. 1) of the unit cell, σ_{ki} are the Cauchy stress components within the bulk region A occupied by the matrix, v_i^* and v_n^* are the Cartesian components and the component normal to the void-surface (measured positive pointing into the bulk material) respectively of an arbitrary kinematically admissible velocity field in A, $\mathbf{x}$ refers to the position of a material point in the current configuration, and k is the curvature of the void-surface S_p (Fig. 1).

Using the interpolation matrices of Eq. (5), the variational statement of Eq. (6) is recast into the following system of nonlinear finite element equations that is to be solved for the vector of displacement increments:

$$\int_A \mathbf{B}_{\mathrm{L}}^{\mathrm{T}} \boldsymbol{\sigma} \,\mathrm{d}A - \int_{S_T} \mathbf{N}_{\mathrm{L}}^{\mathrm{T}} \mathbf{T} \,\mathrm{d}s + \sum_{i=1}^{N_{\mathrm{el}}^{\mathrm{p}}} \gamma_\mathrm{p} \mathbf{p}_i = \mathbf{0}. \tag{7}$$

Here, $\mathbf{T}$ is the vector of externally applied tractions, $N_{\mathrm{el}}^{\mathrm{p}}$ is the number of two-node edges on the void-surface, and $\mathbf{p}_i$ is a vector defined on the ith void-surface element-edge that is completely determined by the

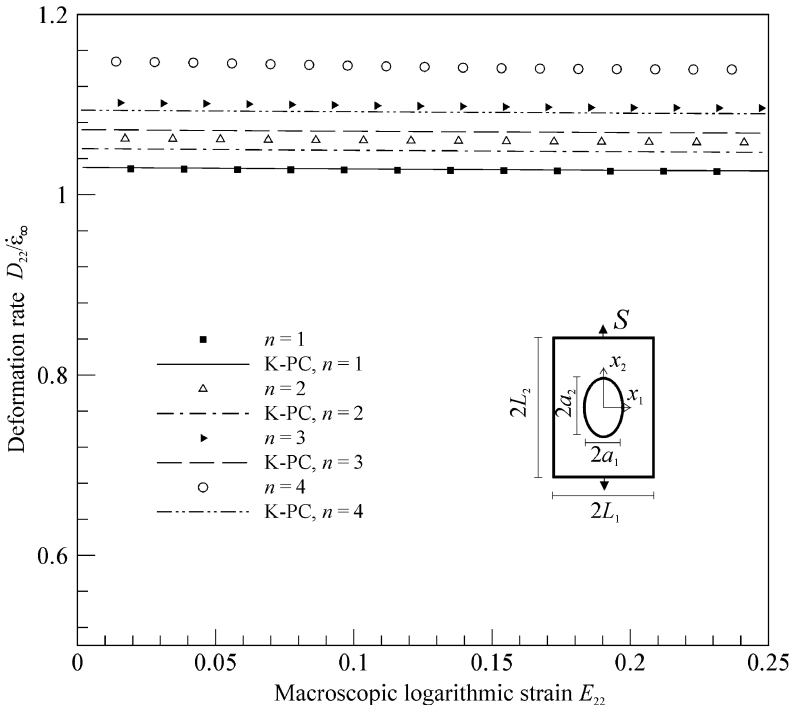

Fig. 4. Macroscopic deformation rate as a function of the creep exponent n: $f_0 = 0.01$, $L_\mathrm{p}/R = 0.01$, and $\psi_\mathrm{p} = 5 \times 10^{-8}$ (no diffusion or surface energy effects). All symbols denote results from the finite-element computations of the present work, and "K–PC" refers to the results obtained using the theory of Kailasam and Ponte Castañeda (1996).

coordinates of the nodes that define that edge (Subramanian and Sofronis, 2001). Given the displacements $\mathbf{u}$, accumulated expansions $\boldsymbol{\alpha}$ at time t_n, and a time increment Δt, Eq. (7) are solved for the displacement increments $\Delta\mathbf{u}$ using a Newton iteration scheme (Subramanian and Sofronis, 2001). The updated displacements $\mathbf{u}+\Delta\mathbf{u}$ are taken as input in the solution to problem (ii) for the expansion increments $\Delta\boldsymbol{\alpha}$ (Subramanian and Sofronis, 2001). Finally, problem (iii) involves computing corrections $d\Delta\mathbf{u}$ to the displacement increments $\Delta\mathbf{u}$ under the constraint that the displacement increment normal to the void-surface be equal to the expansion increments $\Delta\boldsymbol{\alpha}$. Again, problem (iii) ensures that the expansion increments computed on the void-surface are reflected in the displacements in the bulk of the solid, and hence in the computation of the bulk stresses.

4. Numerical results

Following Needleman and Rice (1980), the coupling between the power-law creep deformation in the bulk and the diffusion process over the void surface is expressed in terms of a parameter L_p defined as

$$L_p = \left(\frac{\mathscr{D}_p \gamma_p}{CS^n}\right)^{\frac{1}{4}}. \tag{8}$$

The parameter L_p has dimensions of length; when L_p is large (e.g., large values of $\mathscr{D}_p$ or low values of the applied stress S) compared to the void radius, the surface diffusion process is capable of transporting mass over large distances and hence, is able to neutralize any void-surface curvature gradients set up by the creep

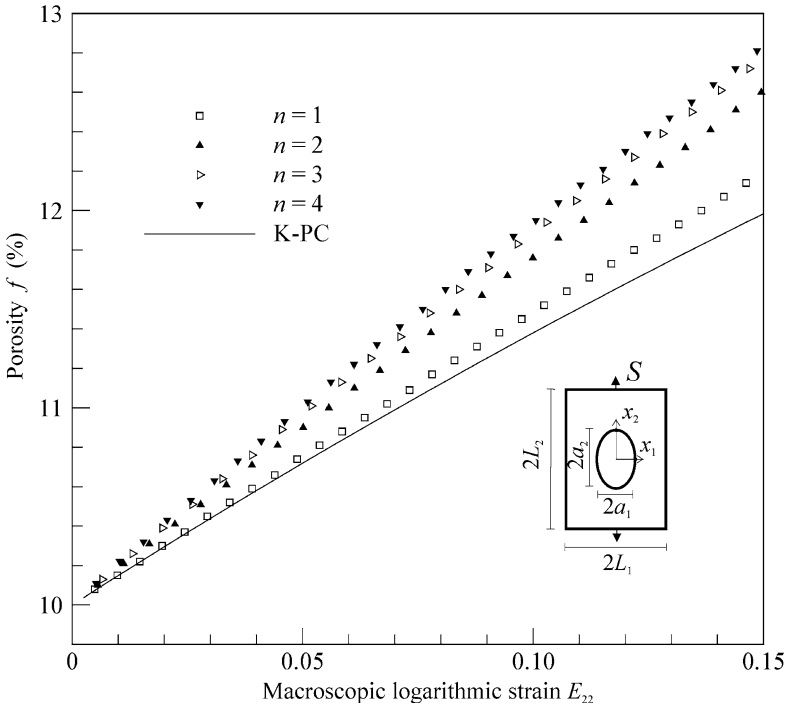

Fig. 5. Evolution of porosity as a function of the creep exponent n: $f_0 = 0.1$, $L_p/R = 0.01$, and $\psi_p = 5\times10^{-8}$ (no diffusion or surface energy effects). All symbols denote results from the finite-element computations of the present work, and "K–PC" refers to the results obtained using the theory of Kailasam and Ponte Castañeda (1996).

deformation in the bulk. On the other hand, when the void radius R is much larger than L_p, mass transport due to surface diffusion is negligible, and does not contribute to the overall deformation of the porous solid. The effect of the void-surface energy on the overall deformation of the voided solid is characterized by the dimensionless group (Subramanian and Sofronis, 2001) ψ_p defined as

$$\psi_p = \frac{\gamma_p}{SR}. \tag{9}$$

If ψ_p is negligibly small ($\psi_p \sim 10^{-8}$) the effect of the void-surface tractions (cf. Eq. (4)) is much smaller than that of the applied stress and the overall deformation is driven by the applied loads. If $\psi_p < 1$ but finite, the surface energy effect can influence the deformation of the void when the magnitude of the void-surface tractions compares to that of the applied stress, e.g., when $\psi_p = 0.5$. When $\psi_p > 1$, the effect of the stresses in the bulk material due to the presence of the void-surface is greater than that of the applied stress, and hence the surface energy effects are expected to dominate the overall deformation, that is, large energy is required to be delivered by the applied loads to change the area of the void surface. The case of $\psi_p = 1$ provides an interesting reference state. For a cylindrical shell subjected to tension on the external surface, and deforming by creep alone under plane-strain conditions, the external tractions are just balanced by the stresses arising from the void when $\psi_p = 1$. The external and internal loads just balance each other, and the displacements are uniformly zero in the shell. If $\psi_p > 1$, the shell expands, and the void grows indefinitely under the influence of the external tension; if $\psi_p < 1$, the surface tension effects are greater, and the void starts to collapse in on itself.

In the following, two sets of calculation results are presented: the first to study the effect of the creep exponent n in the absence of any diffusion and surface energy effects, and the second to quantify the effect

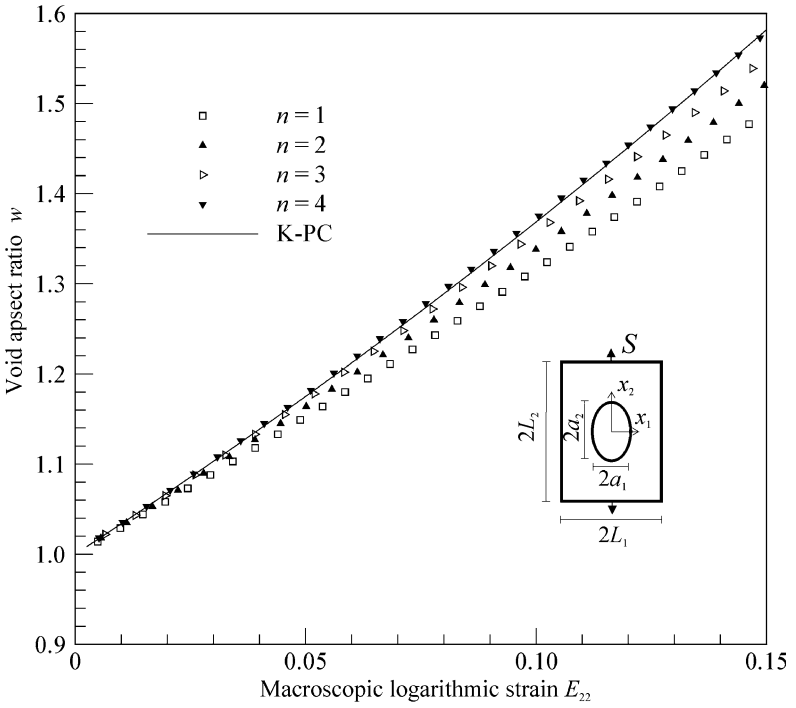

Fig. 6. Evolution of void aspect ratio as a function of the creep exponent n: $f_0 = 0.1$, $L_p/R = 0.01$, and $\psi_p = 5 \times 10^{-8}$ (no diffusion or surface energy effects). All symbols denote results from the finite-element computations of the present work, and "K–PC" refers to the results obtained using the theory of Kailasam and Ponte Castañeda (1996).

of the void-surface diffusion and surface energy on the overall deformation of the unit cell and the evolution of the void shape and size. In each set, the time evolution of deformation was studied using unit cells with f_0 values of 0.01 and 0.1 at time $t = 0$. For each of these geometries, for the classical void growth problem (i.e., no surface diffusion or energy effects), analytical expressions were derived for the macroscopic rate of deformation, as well as f and w using the theory of Kailasam and Ponte Castañeda (1996) as presented in Appendix A and compared with the numerically obtained results. In the legends of the figures to be presented in the remainder of this paper, these theoretical predictions are tagged by the abbreviation "K–PC".

The finite element mesh used in the calculations was made up of 128 eight-noded quadrilateral elements with the element edge increasing radially outward from the void-surface to the loaded boundary. A reduced integration scheme was employed to enforce material incompressibility.

4.1. Effect of creep exponent in the absence of void-surface diffusion and void-surface energy effects

It follows from the celebrated work of Eshelby (1957) that an isolated ellipsoidal void in a linearly creeping solid will always remain an ellipsoid under the action of a uniform stress state at infinity (Budiansky et al., 1982). Hill (1965) has defined the **Q** tensor relating the strain-rate in the isolated void to the remotely applied stresses and established its relationship to the Eshelby tensor **S**. Budiansky et al. (1982) have taken advantage of this result to obtain cavity growth rates in the case of an axisymmetric void in an infinite linearly creeping solid. Recently, Ponte Castañeda and Zaidman (1994) and Kailasam and Ponte Castañeda (1996) have obtained constitutive relations for nonlinearly creeping porous materials with finite porosities taking into consideration the evolution of the porosity f and void aspect ratio in plane and axisymmetric

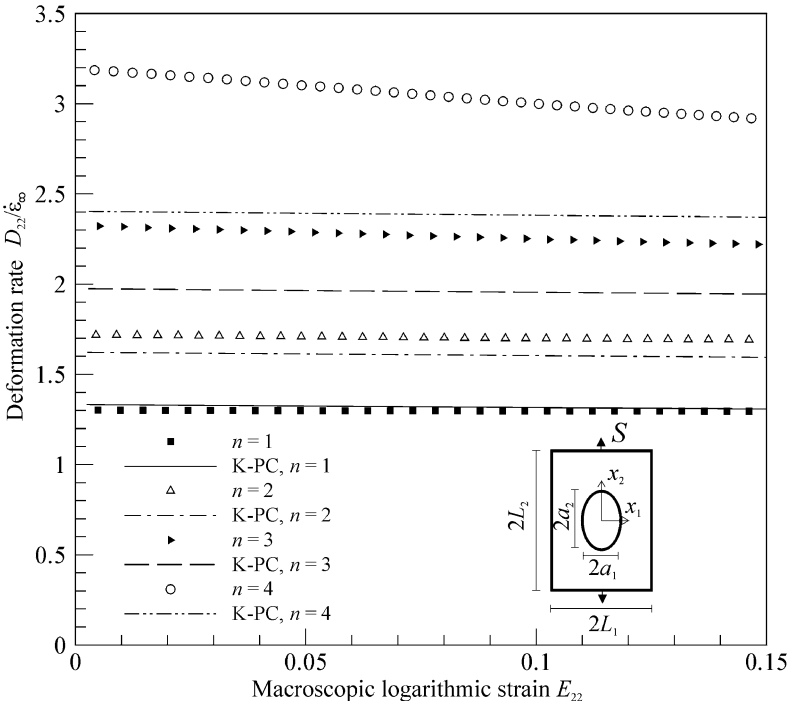

Fig. 7. Macroscopic strain rate as a function of the creep exponent n: $f_0 = 0.1$, $L_p/R = 0.01$, and $\psi_p = 5 \times 10^{-8}$ (no diffusion or surface energy effects). Al symbols denote results from the finite-element computations of the present work, and "K–PC" refers to the results obtained using the theory of Kailasam and Ponte Castañeda (1996).

strain situations (see Appendix A). Their theory recovers the Eshelby theory in the dilute ($f_0 \to 0$) and linear ($n = 1$) limits. Numerical calculations based on the present numerical model with $L_p/R = 0.01$ and $\psi_p = 0.5 \times 10^{-8}$ and which are not reported in this paper for the sake of brevity also recover with an excellent agreement these analytical results (Subramanian, 2001) at these limits ($f_0 = 0.001$ and $n = 1$). Therefore, *the case with* $L_p/R = 0.01$ *and* $\psi_p = 0.5 \times 10^{-8}$ *in the present model was considered to represent void deformation in the absence of surface diffusion and surface energy effects*. The accuracy of the present numerical model was also verified by additional numerical calculations in the nonlinear creep case through comparison (Subramanian, 2001) to results published by Needleman et al. (1995) for axisymmetric void growth in a material with creep exponent of 5. Once again pure power-law creep in the absence of any surface energy or diffusion effects was simulated accurately by setting $L_p/R = 0.01$ and $\psi_p = 0.5 \times 10^{-8}$.

In the first set of calculations, the dimensionless numbers L_p/R and ψ_p were set to 0.01 and 5×10^{-8} respectively in order to make the surface diffusion and surface energy effects negligible, and thus, to isolate the effect of the power-law creep mechanism in the bulk of the solid. The comparison between the numerically obtained evolution of the porosity and the void aspect ratio and those computed from the theory for $f_0 = 0.01$ is illustrated in Figs. 2 and 3. In these and all the following figures wherever applicable, the strain measure used is the logarithmic strain $E_{22} = \log(L_2/L_2|_{t=0})$. The time rates of change of w and f (Appendix Eqs. (A.7) and (A.8)) predicted by the constitutive theory of Kailasam and Ponte Castañeda (1996) depend on the creep exponent in exactly the same manner as do the overall deformation rates (Appendix Eq. (A.4)). As a result, when plotted against a measure of the macroscopic strain, their predictions of f and w for all creep exponents collapse to the same curve. For the case of linear creep ($n = 1$), the theoretical and numerically obtained values of f and w are identical throughout the deformation history. However, as the creep exponent increases, the theoretical pre-

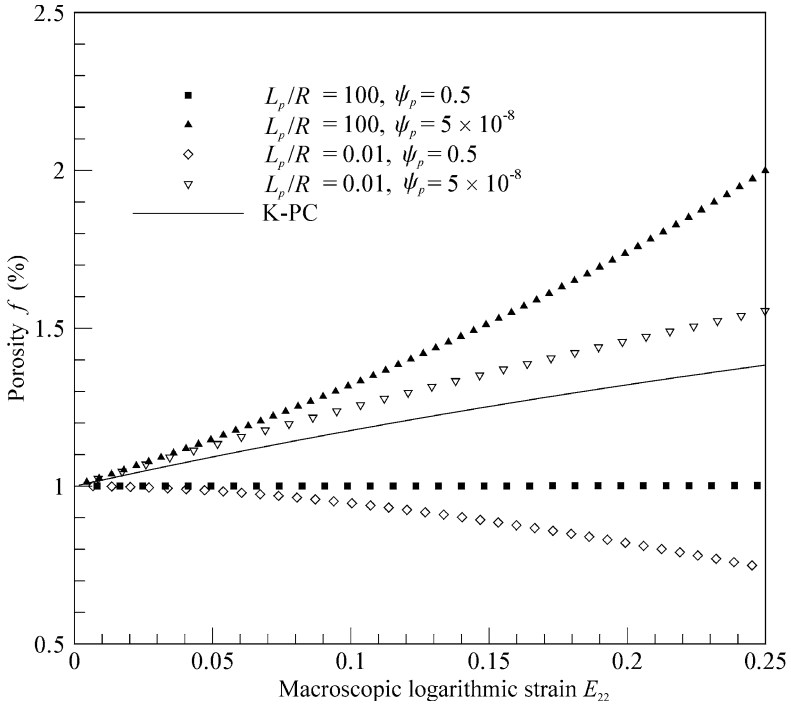

Fig. 8. Evolution of porosity as a function of void-surface characteristics in the presence of diffusion and surface energy effects: $f_0 = 0.01$ and $n = 2$. All symbols denote results from the finite-element computations of the present work, and "K–PC" refers to the results obtained using the theory of Kailasam and Ponte Castañeda (1996).

dictions progressively underestimate both the porosity and the void aspect ratio. As seen from Fig. 3, the void elongates in the direction of the applied load (w increases) for all values of n; in the finite-element results, the higher the creep exponent, the more pronounced is the elongation. Moreover, the rate of change of w increases with deformation for all creep exponents. Simultaneously, the porosity of the solid increases (Fig. 2), but at a rate that decreases with increasing macroscopic strain.

For the same initial porosity, Fig. 4 shows the numerically computed macroscopic deformation rates in the loading direction compared with the corresponding theoretical predictions. Here, the normalizing strain rate is $\dot{\varepsilon}_\infty = (\sqrt{3}/2)^{(n+1)} CS^n$, which results when the pure matrix material is subjected to the same plane-strain loading conditions. For all creep exponents considered, the overall response of the cell is softer than that of the void-free material (i.e. $D_{22}/\dot{\varepsilon}_\infty > 1$). Both the numerical computations and the theory predict more pronounced softening of the solid with increasing creep exponent. The numerically computed deformation rates are in perfect agreement with the theoretical predictions for a linearly creeping material; but for higher creep exponents, the theory of Kailasam and Ponte Castañeda (1996) predicts a stiffer overall response than seen in the numerical computations. The variation of the normalized deformation rate with strain is negligible for all creep exponents considered.

The corresponding trends for a solid with an initial porosity of 0.1 are shown in Figs. 5–7. Values of f computed using the theoretical approach of Kailasam and Ponte Castañeda (1996) underestimate the numerically obtained values, just as in the case of initial porosity 0.01. However, the theoretical predictions for w agree very well with the values of the present model for $n = 4$, while significantly overestimating the aspect ratio for other creep exponents. For the $f_0 = 0.01$ case (Fig. 3), the K–PC results for the evolution of the aspect ratio w with strain agree well with the numerical results for $n = 1$. On the other hand, for the

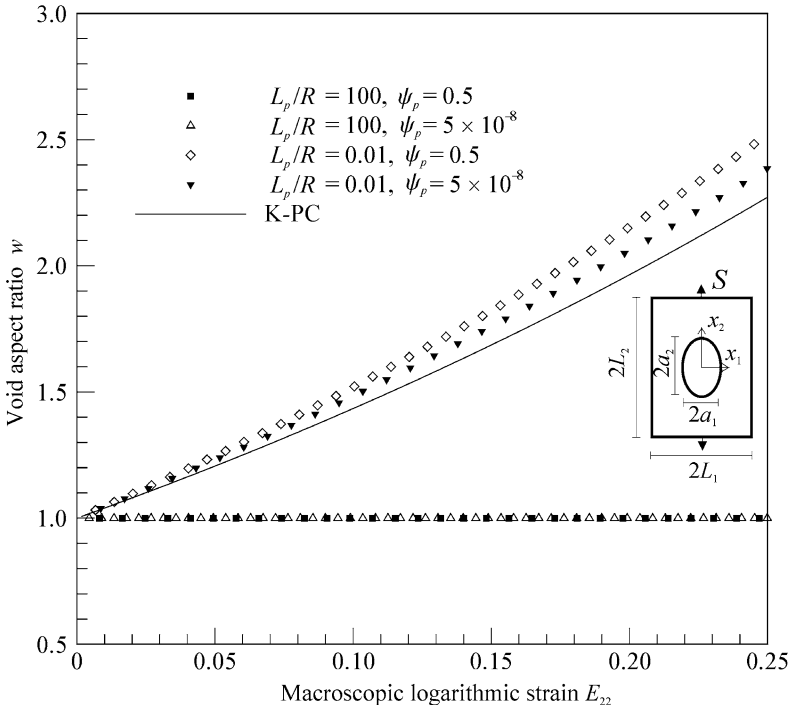

Fig. 9. Evolution of aspect ratio of an initially circular void as a function of void-surface characteristics in the presence of diffusion and surface energy effects: $f_0 = 0.01$ and $n = 2$. All symbols denote results from the finite-element computations of the present work, and "K–PC" refers to the results obtained using the theory of Kailasam and Ponte Castañeda (1996).

$f_0 = 0.1$ case (Fig. 6) the K–PC results for w agree well with the $n = 4$ numerical results. The apparent discrepancy between the two cases is due to the fact that when plotted against strain, the K–PC curve shows no sensitivity on the creep exponent, whereas the numerical results do. Certainly, unlike the K–PC results, the numerical results do depend on the initial porosity studied.

Lastly, both the K–PC model and the present model predict a much softer macroscopic response for the voided solid at this porosity level ($f_0 = 0.1$). However, the discrepancy between the theoretical values and those of the finite-element calculations persists, and is once again the most for $n = 4$. It is interesting to note that for $n = 4$, the macroscopic deformation rate shows a noticeable decrease with strain (Fig. 7), a trend not observed for any other combination of creep exponent and initial porosity.

4.2. Effect of void-surface energy and void-surface diffusion

In order to study the effect of the void-surface energy and the surface diffusion process on void growth, a second set of computations was performed employing the same two initial porosity values. The creep exponent n was fixed at 2, and in order to investigate a wide range of surface energy and diffusion effects, L_p/R was set to either 0.01 (no surface diffusion) or 100 (extremely fast surface diffusion), and ψ_p to either 5×10^{-8} (negligible surface energy effects) or 0.5 (significant surface energy effects). Values of ψ_p greater than unity were seen to be difficult from a computational standpoint leading to very slow convergence of the three-step iterative scheme, and were therefore not pursued. As in the previous subsection, computed results were compared with those of the theory of Ponte Castañeda and co-workers in the absence of void-surface diffusion or surface energy effects.

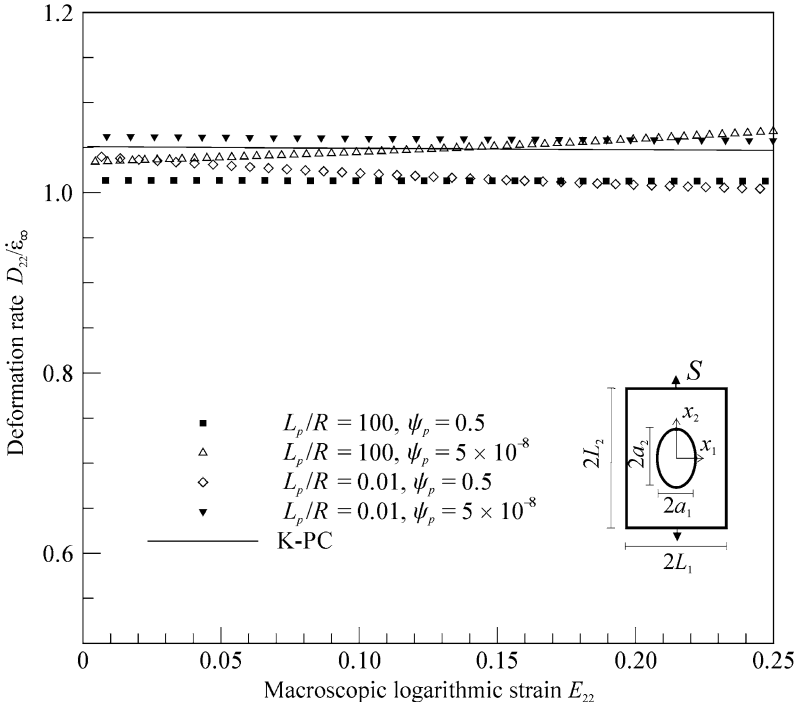

Fig. 10. Macroscopic deformation rate as a function of void-surface characteristics in the presence of diffusion and surface energy effects: $f_0 = 0.01$ and $n = 2$. All symbols denote results from the finite-element computations of the present work, and "K–PC" refers to the results obtained using the theory of Kailasam and Ponte Castañeda (1996).

Computed porosity and aspect ratio values for the four combinations of L_p/R and ψ_p for the case of $f_0 = 0.01$ are shown in Figs. 8 and 9 along with the theoretical predictions. The four material systems exhibit distinct trends. $L_p/R = 0.01$ and $\psi_p = 5 \times 10^{-8}$ correspond to the "classical void growth" problem, wherein both surface diffusion and surface energy effects are neglected, and the only deformation mechanism is power-law creep in the bulk. Under these conditions, the porosity monotonically increases with macroscopic deformation (Fig. 8) and the applied load continuously elongates the void in its direction (Fig. 9). When $L_p/R = 100$ and $\psi_p = 5 \times 10^{-8}$, we have a system which is different from the classical void growth systems only in that there is very rapid surface diffusion over the void-surface. From Fig. 8, it is clear that the porosity increases at a rate that increases with macroscopic strain in this case, and the corresponding curve on Fig. 9 shows that the void always remains circular. Evidently, the very fast surface diffusion neutralizes the curvature gradient set up by the bulk deformation. On the other hand, the case of $L_p/R = 0.01$ and $\psi_p = 0.5$ (very high surface energy effect, but very slow surface diffusion) is a rather intriguing one. The void shrinks in the transverse direction with increasing macroscopic strain (Fig. 9)—the void shapes are similar to those of the classical case of void growth i.e., with negligible surface diffusion and energy effects—but since the surface energy effect is quite high, increasing the void-surface area is energetically expensive, and as a result the porosity decreases with time (Fig. 8). Finally, when surface diffusion is extremely fast, and there are significant surface energy effects ($L_p/R = 100$ and $\psi_p = 0.5$), the porosity does not change, nor does the aspect ratio. The void maintains its shape throughout the course of deformation, and the bulk material flows around it under the influence of the external loads. In general, the void aspect ratio evolution (Figs. 9 and 12) for the four cases falls into either of two categories—when surface diffusion is extremely fast, $L_p/R = 100$, the void remains a circle, whereas w increases at an ever-increasing

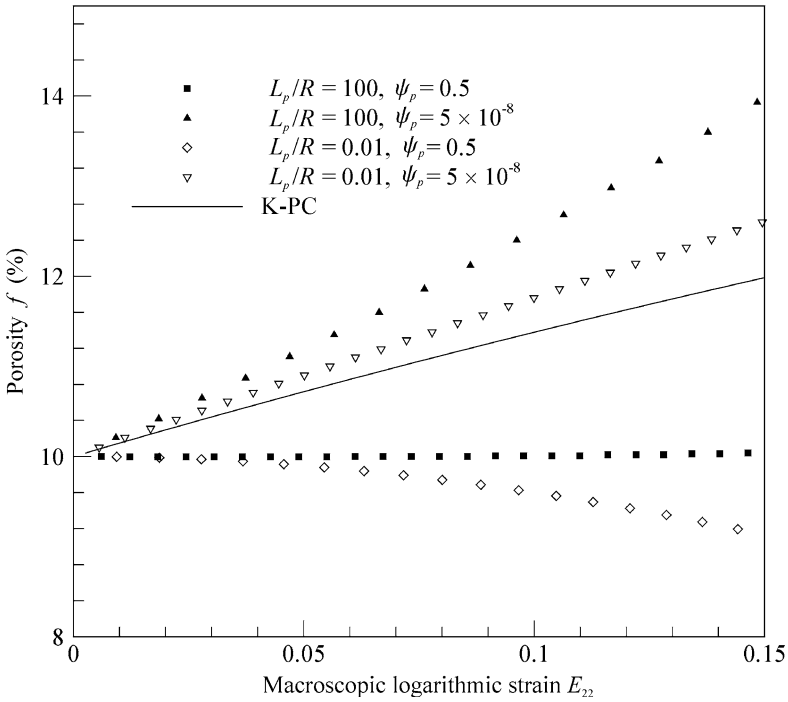

Fig. 11. Evolution of porosity as a function of void-surface characteristics in the presence of diffusion and surface energy effects: $f_0 = 0.1$ and $n = 2$. All symbols denote results from the finite-element computations of the present work, and "K–PC" refers to the results obtained using the theory of Kailasam and Ponte Castañeda (1996).

rate with macroscopic strain when surface diffusion effects are negligible, $L_p/R = 0.01$. Exactly the same trends are observed for f and w when $f_0 = 0.1$ (Figs. 11 and 12).

The macroscopic deformation rates for the four combinations of L_p/R and ψ_p for $f_0 = 0.01$ are shown in Fig. 10. When both surface energy and surface diffusion effects are absent ($L_p/R = 0.01$ and $\psi_p = 5 \times 10^{-8}$), the voided solid is softer than a void-free one ($D_{22}/\dot{\varepsilon}_\infty > 1$), and the deformation rate does not appear to have any dependence on the magnitude of the macroscopic deformation. When the surface energy effect is negligible ($\psi_p = 5 \times 10^{-8}$) but the free surface diffusion is rapid ($L_p/R = 100$), the solid is softer than the void-free material to begin with, and continues to progressively soften with increasing strain. On the other hand, if the classical void is replaced by one with significant surface energy effects ($L_p/R = 0.01$, $\psi_p = 0.5$), the deformation rate shows an interesting trend. Even though the solid is softer than the void-free solid initially, it hardens with deformation, and the voided solid behaves like the void-free solid at a macroscopic strain of 25%. The final case shown in Fig. 10 is when $L_p/R = 100$ and $\psi_p = 0.5$ (extremely fast surface diffusion over a void-surface that is energetically expensive to deform); here, the macroscopic deformation rate remains constant with deformation, as do the previously-discussed porosity and aspect-ratio. From these curves, it appears that the surface energy parameter has more influence on the overall deformation rates: the higher the surface energy parameter, the harder the voided material behaves. The surface diffusion parameter certainly affects deformation rates, but its effect is secondary to that of the surface energy parameter. The corresponding deformation rate plots for $f_0 = 0.1$ are shown in Fig. 13. The trends in this plot are the same as in the $f_0 = 0.01$, but the differences in deformation rates for the four cases shown are significantly larger.

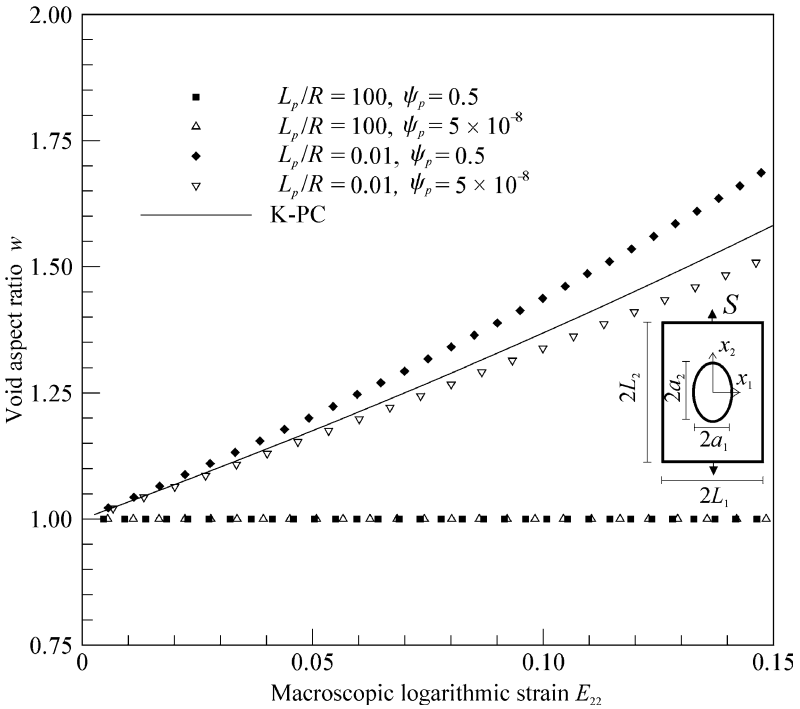

Fig. 12. Evolution of aspect ratio of an initially circular void as a function of void-surface characteristics in the presence of diffusion and surface energy effects: $f_0 = 0.1$ and $n = 2$. All symbols denote results from the finite-element computations of the present work, and "K–PC" refers to the results obtained using the theory of Kailasam and Ponte Castañeda (1996).

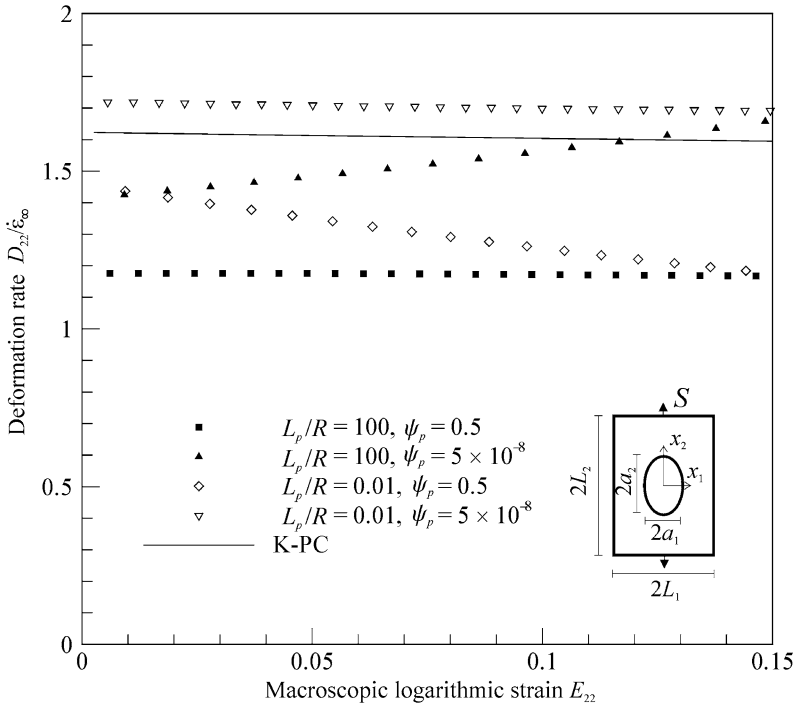

Fig. 13. Macroscopic deformation rate as a function of void-surface characteristics in the presence of diffusion and surface energy effects: $f_0 = 0.1$ and $n = 2$. All symbols denote results from the finite-element computations of the present work, and "K–PC" refers to the results obtained using the theory of Kailasam and Ponte Castañeda (1996).

5. Discussion

The present computations indicate that when surface energy and surface diffusion effects are negligible, initial porosity and the nonlinearity of creep deformation of the matrix significantly affect the overall response of voided materials. In line with expectations, when void-surface effects can be ignored, materials with higher porosity are softer than the corresponding void-free materials, and the macroscopic softening relative to the corresponding void-free material is more for material whose creep exponent is higher. Computations indicate that the theory of Ponte Castañeda and co-workers performs very well in predicting the macroscopic response of voided materials at relatively low porosities (Fig. 4). For an initial porosity of 0.1, the theoretical predictions of Kailasam and Ponte Castañeda (1996) are still quite acceptable for low creep exponents (see Fig. 7) although the discrepancy between the theoretical predictions and computed values is approximately 25% for $n = 4$. For all cases except that of a linear material with very low initial porosity, the theory underestimates the evolving porosity (Figs. 2 and 5). At an initial porosity $f_0 = 0.01$, the theoretical predictions of the void aspect ratio are more accurate for the lower creep exponent (Fig. 3), whereas at an initial porosity $f_0 = 0.1$, the predictions are more accurate at higher creep exponents (Fig. 6).

Consideration of void shape changes throughout the course of straining serves as an aid in rationalizing the observed effects of the void-surface tractions and void-surface diffusion process. Figs. 14–17 show the void profiles at different stages of macroscopic straining for the four combinations of surface diffusion and surface energy effects discussed in the previous section when $f_0 = 0.001$. Each set of profiles is strikingly different from any of the others.

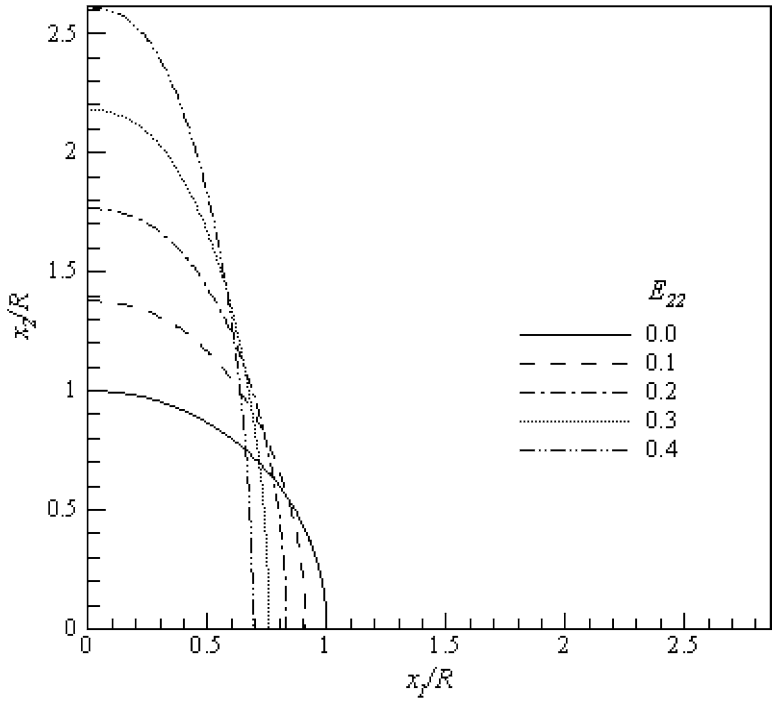

Fig. 14. Void profiles at various stages of straining in the presence of diffusion and surface energy effects: $f_0 = 0.001$, $L_p/R = 0.01$, $\psi_p = 5 \times 10^{-8}$, and $n = 2$. This case of very slow surface diffusion and very small surface energy effects corresponds to "classical" void growth studies in which the void-surface was traction-free.

In the case of low L_p/R and ψ_p (i.e., $L_p/R = 0.01$, $\psi_p = 5 \times 10^{-8}$), since the diffusion process is much slower than the creep in the matrix, the distortions set up by the latter persist; further, such distortions are energetically inexpensive due to the low ψ_p value. Progressive elongation of the void in the loading direction (Fig. 14) ensues, as the void continues to align itself parallel to the applied load. If the surface energy parameter ψ_p is extremely low, $\psi_p = 5 \times 10^{-8}$, and surface diffusion is very fast, $L_p/R = 100$, (Fig. 15), the void retains its circular shape but steadily increases in size, resulting in continuously increasing porosity. When the surface diffusion process is extremely fast, changes in curvature are quickly neutralized and thus, the void resists distortion of its shape. Since the applied load is not capable of elongating the void along the loading direction, the solid exhibits enhanced transverse strength. As the void radius increases and the lateral face of the unit cell is drawn in to maintain creep incompressibility, the load-bearing ligament shrinks leading to the progressively increasing macroscopic deformation rates as those seen in Figs. 10 and 13 for porosities 0.01 and 0.1, respectively.

For very slow surface diffusion and very high surface energy parameter ($L_p/R = 0.01, \psi_p = 0.5$), one observes (Fig. 16) that even though the void is free to change its shape, changing its area is not feasible because the surface energy is extremely high in relation to the applied load and void size, making such changes energetically very expensive. As the macroscopic straining continues, curvature gradients become more severe, with the curvature at the pole of the void increasing constantly (surface becoming more curved locally), while that at the equator decreases continuously. Once the curvature at the pole reaches a high enough value, it becomes prohibitively expensive from an energetic standpoint to increase the void area by moving the pole of the void in the loading direction. As a result, the void effectively locks up at the pole even though the solid itself continues to deform. At the equator, the void-surface still moves inwards,

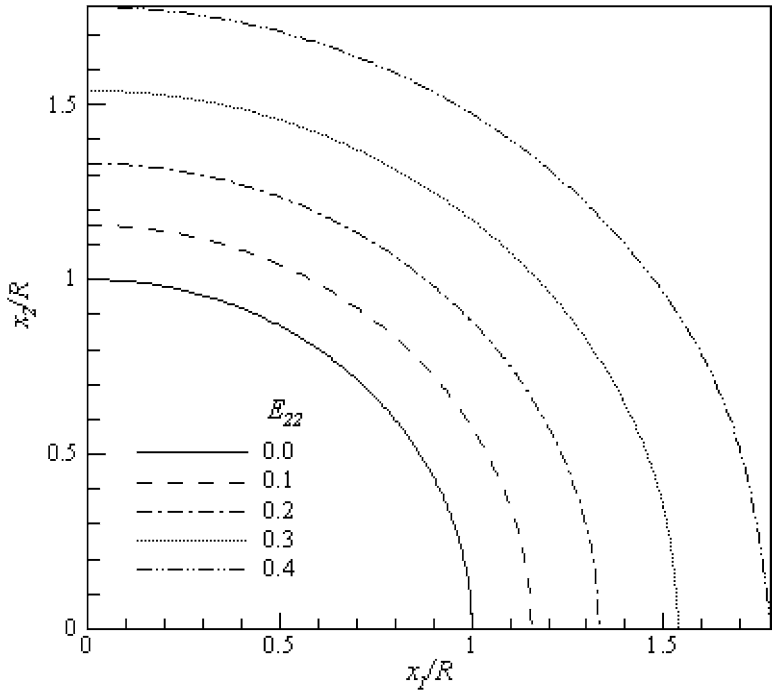

Fig. 15. Void profiles at various stages of straining in the presence of rapid surface diffusion and small surface energy effects: $f_0 = 0.001$, $L_p/R = 100$, $\psi_p = 5 \times 10^{-8}$, and $n = 2$.

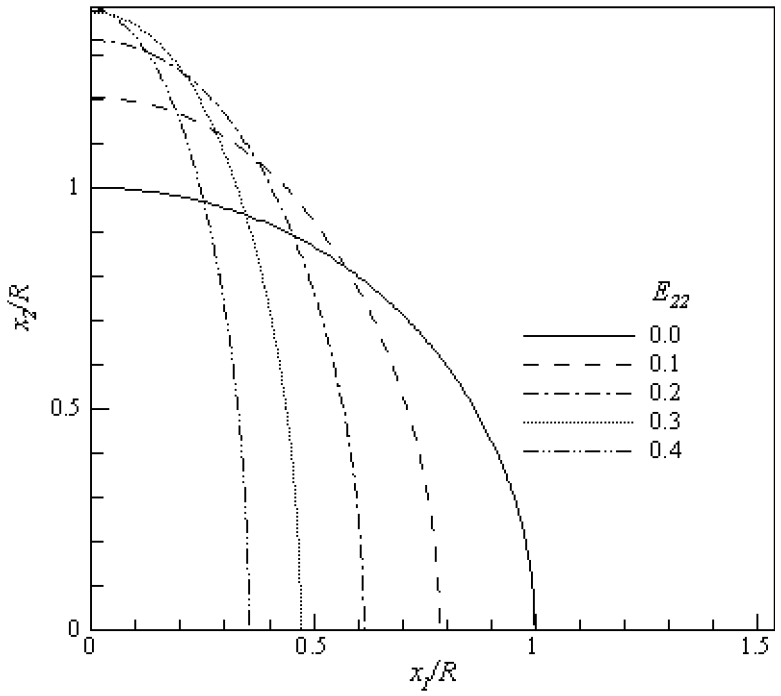

Fig. 16. Void profiles at various stages of straining in the presence of very slow surface diffusion and strong surface energy effects: $f_0 = 0.001$, $L_p/R = 0.01$, $\psi_p = 0.5$, and $n = 2$.

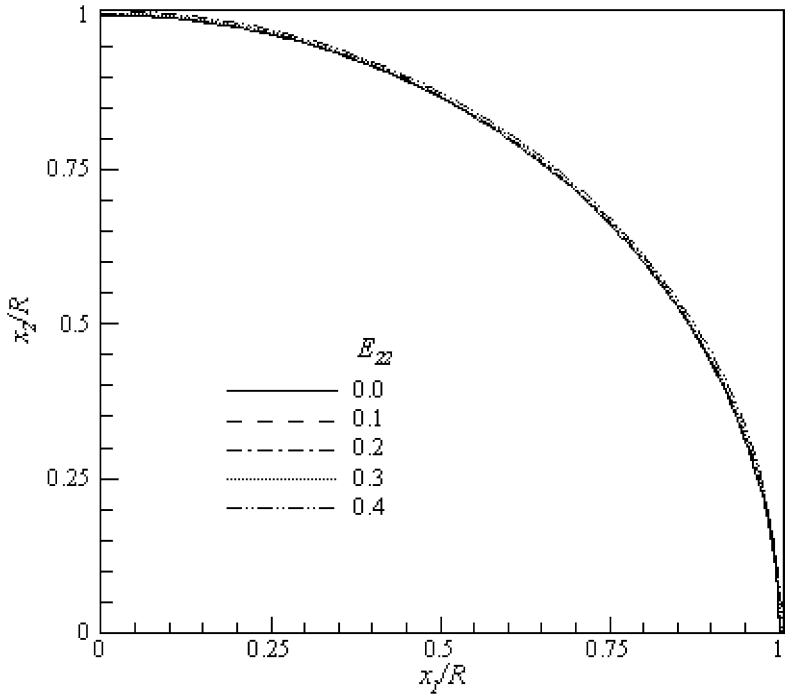

Fig. 17. Void profiles at various stages of straining in the presence of both rapid diffusion and strong surface energy effects: $f_0 = 0.001$, $L_p/R = 100$, $\psi_p = 0.5$, and $n = 2$.

decreasing the cross-sectional area of the void leading to decreasing porosity as shown in Figs. 8 and 11, and increasing aspect ratio as shown in Figs. 9 and 12. As the void area shrinks, further deformation of the void becomes progressively difficult leading to decreasing overall deformation rates as in Figs. 10 and 13.

When the diffusion process over the void is capable of transporting mass over large distances compared to the void radius and the changes to the void length (i.e. area per unit length in the 3-direction) are energetically very expensive ($L_p/R = 100, \psi_p = 0.5$), the void-surface shows extremely small amount of deformation (Fig. 17) even at a macroscopic strain of 0.4. One is then left with an almost incompressible void in an incompressible matrix resulting in constant porosity at all stages of macroscopic straining. As seen in Figs. 10 and 13, the normalized macroscopic deformation rate is also constant, although it increases as the initial porosity of the solid increases. Macroscopically, the behaviors of the solid with such a void and a solid block of the same material are very much alike, with the only observable difference being in the magnitude of the deformation rate.

For all the cases of initial porosity studied, computations were not pursued beyond the range of E_{22} shown in the plots due to mesh distortion at large deformations of the unit cell. The range of E_{22} shown decreases with increasing initial porosity for the obvious reason that mesh distortion becomes more pronounced for larger values of f_0. Based on the trends shown in Figs. 10 and 13, it appears that the normalized macroscopic deformation rate $D_{22}/\dot{\varepsilon}_\infty$ may fall below 1 for a material with $L_p/R = 0.01$ and $\psi_p = 0.5$ at macroscopic strains larger than the ones shown. Thus, one arrives at the following interesting and surprising result: at large enough strains, a solid with a high void-surface energy parameter will be harder to deform than a void-free solid, i.e. such a void acts as a reinforcement. Further, it is the interaction of

the void-surface energy effect with the creep deformation in the matrix that acts as the reinforcing mechanism. Recall that surface diffusion is extremely slow in this case, and therefore it does not contribute to the observed behavior.

Comparing Figs. 10 and 13, in which the only difference in inputs is the initial porosity, one clearly sees that increasing porosity augments the effect of surface energy on void growth. In fact, at higher porosity, the deformation rates are higher for every combination of L_p/R and ψ_p studied. Both Figs. 10 and 13 show an appreciable decrease of the macroscopic deformation rate when $\psi_p = 0.5$ and $L_p/R = 0.01$. It is interesting that in the absence of any void-surface energy or diffusion effects (see Fig. 7 for $f_0 = 0.1$) the macroscopic deformation rate also shows a decrease for all creep exponents, with the decrease being most noticeable for $n = 4$. Comparing the macroscopic deformation rates for $n = 2$, one clearly sees from Fig. 13 that with $L_p/R = 0.01$ and $\psi_p = 0.5$ the effect of decreasing deformation rate is significantly magnified relatively to the case of no void-surface energy or diffusion effects. Thus, regarding the interaction between the surface energy effect and the creep exponent, one may infer the following: (i) there is a slight decrease in deformation rate i.e. the porous solid hardens slightly with strain, with the amount of hardening increasing with creep exponent; (ii) there is a much sharper decrease when the surface energy effects are very high and surface diffusion is very slow. In short, the creep exponent modulates the surface energy effect slightly.

It can be said that in a voided material with a large surface energy parameter ψ_p the tractions acting on the void-surface compete with the externally applied loads on deforming the void. This mechanism of internal tractions, which is absent in the homogeneous material case, may over-ride the external loads tending to enlarge the void, thus leading to the "surprising" result of void shrinkage. Using strain gradient plasticity in rate independent solids, Fleck and Hutchinson (1997) and Liu et al. (2003) found that nanosized voids are very hard to enlarge in comparison to micron-sized voids. Ahn et al. (2005) investigating void growth by dislocation loop emission found that the smaller the void radius, the larger the external load required for the punching out of the loops from the void-surface due to the larger image stress and surface energy effect resisting the emission of the loops as the void radius decreases. A similar result was also reached by Lubarda et al. (2004) in the case of single edge dislocations emitted from a void. Thus, by associating the large surface energy parameter ψ_p to a small void radius R (Eq. (9)), one concludes that the present study's result on void shrinkage is in line with the increased resistance to deformation observed in the case of nanosized voids in continuum and dislocation plasticity studies of void growth.

The present numerical-model approach to the study of the effects of void-surface energy and void-surface diffusion on void growth is extremely relevant to many technological applications involving high temperature deformation. By way of example, one may mention the diffusive cavitation of grain-boundaries by creep deformation at high temperatures. The celebrated work of Needleman and Rice (1980) analyzed void growth based on equilibrium void-shapes resulting from extremely fast void-surface diffusion while it ignored void-surface curvature effects. Another field of application of the present model is the deformation of sintered/compacted solids with closed porosities. An extended literature review on the pertinence of the void-surface effects on powder sintering can be found in the work of Subramanian and Sofronis (2001).

6. Closure

The finite deformation of a power-law creeping material containing initially circular voids has been studied using the finite-element method under plane-strain tension. The effect of initial porosity and creep exponent on the microstructural variables, as well as the overall macroscopic deformation rate have been quantified for the case of negligible void-surface energy and diffusion effects. The theory of Kailasam and Ponte Castañeda (1996) has been shown to perform quite well for low porosities and low creep exponents, while at higher initial porosities and creep exponent values, the theory still yields acceptable results.

Void growth at high temperatures is affected by the competing action of nonlinear creep deformation in the surrounding matrix and surface diffusion driven by void-surface curvature gradients. Finite element analysis of the coupled problem indicates that microstructural variables (porosity and void aspect ratio), as well as macroscopic deformation rates are strongly affected by the relative strengths of the void-surface energy effect and void-surface diffusion process vis-a-vis the rate of creep deformation in the bulk of the solid. A rich variety of solutions has been revealed, and which solution is obtained for a given material, loading conditions, and geometry depends on the strength of the void-surface diffusion and surface energy effect relative to the applied load and the creep deformation characteristics of the matrix material. It should be pointed out that the classical void growth models which ignore both the surface energy and surface diffusion effects recover only one branch of the solutions revealed by the present study. In essence, the diffusion process controls the shape of the void: if diffusion is fast, the void is always circular; if it is extremely slow, the void is free to elongate along the loading direction. On the other hand, the size changes of the void are determined by the surface energy parameter: if ψ_{p} is small (energetically inexpensive to effect void-surface area changes), the void is free to expand, whereas a high value of ψ_{p} places a high price on increases in void size.

The evolution of void shape and size corresponds directly to distinct macroscopic deformation patterns. When void-surface diffusion is extremely fast, along with a high surface energy parameter, the void does not deform even at large macroscopic strains, resulting in a steady state macroscopic deformation rate that depends only on the initial porosity. In the case of significant surface energy effects with an accompanying slow surface diffusion process, the voided material becomes progressively stiffer macroscopically due to increasing difficulty in distorting the void, leading possibly to the surprising scenario of voids acting as reinforcement. Interestingly, in this case, the voided material may become stronger than the void-free material at large enough macroscopic strains. When both surface energy and surface diffusion effects are negligible, the void grows stably in the loading directions and the macroscopic deformation rate increases with increasing initial porosity. Lastly, for the case of very fast surface diffusion and negligible surface energy effects, the void expands in all directions despite the fact that loading is uniaxial. Further, the voided solid continues to soften macroscopically as the porosity steadily increases.

Acknowledgement

This work was supported by the Department of Energy under grant DEFGO6-96ER45439 and by the National Science Foundation under grant DMR0302470.

Appendix A. Void growth in a creeping solid under plane-strain conditions with no surface diffusion or surface energy effects

One can calculate the effective compliance $\overline{\mathbf{M}}$ of a linearly creeping porous solid as a function of its porosity through (Kailasam and Ponte Castañeda, 1996)

$$\overline{\mathbf{M}} = \left\{ \mathbf{I} + \frac{f}{1-f} (\mathbf{I} - \mathbf{S})^{-1} \right\} \mathbf{M}, \tag{A.1}$$

where $\mathbf{I}$ is the identity tensor, $\mathbf{M}$ is the matrix compliance tensor (inverse of the stiffness tensor), $\mathbf{S}$ is the Eshelby tensor and f is the porosity. For the case of plane strain deformation of a linearly creeping material (whose creep modulus is μ) with an initially circular void, the above expression yields

$$\overline{\mathbf{M}} = \frac{1}{6\mu(1-f)} \begin{bmatrix} 2+3fw & -1 & -1 & 0 \\ -1 & \dfrac{3f+2w}{w} & -1 & 0 \\ -1 & -1 & 2 & 0 \\ 0 & 0 & 0 & \dfrac{3f+6w+3fw^2}{2w} \end{bmatrix}. \tag{A.2}$$

The above effective compliance of the linear material is used to compute the constitutive response of the nonlinearly creeping solid with voids. Specifically, the effective potential $\overline{U}(\bar{\boldsymbol{\sigma}})$ (Kailasam and Ponte Castañeda, 1996) for the nonlinearly viscous porous material is calculated in terms of the material-independent tensor $\bar{\mathbf{m}} = 3\mu\overline{\mathbf{M}}$ to be

$$\overline{U}(\bar{\boldsymbol{\sigma}}) = \frac{1}{3\mu(n+1)} \left(\frac{1}{1-f}\right)^{\frac{n-1}{2}} \left[\bar{\boldsymbol{\sigma}}^{\mathrm{T}} \bar{\mathbf{m}} \bar{\boldsymbol{\sigma}}\right]^{\frac{n+1}{2}}, \tag{A.3}$$

from which the effective rate of deformation of the porous solid is derived through the relation $\overline{\mathbf{D}} = \partial\overline{U}/\partial\bar{\boldsymbol{\sigma}}$. Thus, for the macroscopic straining considered in this work, the theory of Kailasam and Ponte Castañeda (1996) yields the following average deformation rates:

$$\begin{aligned} \overline{D}_{11} &= -\left(\frac{3}{4}\right)^{\frac{n+1}{2}} CS^n \frac{1}{(1-f)^n} \left(1+\frac{2f}{w}\right)^{\frac{n-1}{2}}, \\ \overline{D}_{22} &= \left(\frac{3}{4}\right)^{\frac{n+1}{2}} CS^n \frac{1}{(1-f)^n} \left(1+\frac{2f}{w}\right)^{\frac{n+1}{2}}, \\ \overline{D}_{12} &= \overline{D}_{33} = 0. \end{aligned} \tag{A.4}$$

The rate of deformation inside the voids is related to the overall rate of deformation through the so-called strain-rate concentration tensor $\mathbf{A}^{\mathrm{v}}$, such that $\mathbf{D}^{\mathrm{v}} = \mathbf{A}^{\mathrm{v}}\overline{\mathbf{D}}$. Kailasam and Ponte Castañeda (1996) report $\mathbf{A}^{\mathrm{v}}$ for a porous solid to be

$$\mathbf{A}^{\mathrm{v}} = [\mathbf{I} - (1-f)\mathbf{S}]^{-1}, \tag{A.5}$$

the use of which in conjunction with the relationship of the previous sentence and Eq. (A.4) yields the rate of deformation in the void as

$$\begin{aligned} D^{\mathrm{v}}_{11} &= -\left(\frac{3}{4}\right)^{\frac{n+1}{2}} CS^n \frac{1}{(1-f)^n} \left(1+\frac{2f}{w}\right)^{\frac{n-1}{2}}, \\ D^{\mathrm{v}}_{22} &= \left(\frac{3}{4}\right)^{\frac{n+1}{2}} CS^n \frac{1}{(1-f)^n} \left(1+\frac{2f}{w}\right)^{\frac{n+1}{2}} \left(\frac{2+w}{2f+w}\right), \\ D^{\mathrm{v}}_{12} &= D^{\mathrm{v}}_{33} = 0. \end{aligned} \tag{A.6}$$

Since the void aspect ratio changes with time according to the relation $\dot{w} = w(D^{\mathrm{v}}_{22} - D^{\mathrm{v}}_{11})$, and creep incompressibility dictates that $\dot{f} = f(1-\overline{D}_{kk})$, one arrives at the following system of coupled ordinary differential equations for f and w:

$$\dot{w} = 2\left(\frac{3}{4}\right)^{\frac{n+1}{2}} CS^n \frac{1+w}{(1-f)^n} \left(1+\frac{2f}{w}\right)^{\frac{n-1}{2}}, \tag{A.7}$$

and

$$\dot{f} = 2\left(\frac{3}{4}\right)^{\frac{n+1}{2}} CS^n \frac{f}{w(1-f)^{n-1}} \left(1+\frac{2f}{w}\right)^{\frac{n-1}{2}}. \tag{A.8}$$

Note that from Eq. (A.7), the evolution equation for w for the case of a hole in an infinite, linearly viscous medium ($f \to 0$, and $n = 1$) reduces to

$$\dot{w} = \frac{3CS}{2}(1+w). \tag{A.9}$$

References

Ahn, D.C., Sofronis, P., Minich, R., 2005. On the micromechanics of void growth by dislocation loop emission. J. Mech. Phys. Solids, to appear.

Budiansky, B., Hutchinson, J.W., Slutsky, S., 1982. Void growth and collapse in solids. In: Hopkins, H.G., Sewell, M.J. (Eds.), Mechanics of Solids—The Rodney Hill 60th Anniversary Volume. Pergamon Press, pp. 13–45.

Chuang, T.-Z., Kagawa, I.K., Rice, J.R., Sills, L.B., 1979. Non-equilibrium models for diffusive cavitation of grain interfaces. Acta Metal. 27 (3), 265–284.

Eshelby, J.D., 1957. The determination of the elastic field of an ellipsoidal inclusion, and related problems. Proc. Roy. Soc. Lond. A 241, 376–396.

Fleck, N.A., Hutchinson, J.W., 1997. Strain gradient plasticity. In: Hutchinson, J.W., Wu, T.Y. (Eds.), Advances in Applied Mechanics, vol. 33. Academic Press, New York, pp. 295–361.

Freund, L.B., Beltz, G.E., Jonsdottir, F., 1993. Continuum modeling of stress-driven surface diffusion in strained elastic materials. Mater. Res. Soc. Symp. Proc. 308, 383–394.

Golaganu, M., Leblond, J.-B., Devaux, J., 1993. Approximate models for ductile metals containing non-spherical voids—Case of axisymmetric prolate ellipsoidal cavities. J. Mech. Phys. Solids 41, 1723–1754.

Golaganu, M., Leblond, J.-B., Devaux, J., 1994. Approximate models for ductile metals containing non-spherical voids—Case of axisymmetric oblate ellipsoidal cavities. J. Engng. Mater. Technol. 61, 236–242.

Gurtin, M.E., Murdoch, A.I., 1975. A continuum theory of elastic material surfaces. Arch. Rat. Mech. Anal. 57 (4), 291–323.

Herring, C., 1951. Surface tension as a motivation for sintering. In: The Physics of Powder Metallurgy—A Symposium Held at Bayside, L.I., New York, August 24–26, 1949. pp. 143–179.

Hill, R., 1965. A self-consistent mechanics of composite materials. J. Mech. Phys. Solids 13 (4), 213–222.

Kailasam, M., Ponte Castañeda, P., 1996. Constitutive relations for porous materials: the effect of changing void shape and orientation. In: Pineau, A., Zaoui, A. (Eds.), UTAM Symposium on Micromechanics of Plasticity and Damage of Multiphase Materials. pp. 215–222.

Kailasam, M., Aravas, N., Ponte Castañeda, P., 2000. Porous metals with developing anisotropy: constitutive models, computational issues and applications to deformation processing. CMES 1 (2), 105–118.

Lubarda, V.A., Schneider, M.S., Kalantar, D.H., Remington, B.R., Meyers, M.A., 2004. Void growth by dislocation emission. Acta Mater. 52, 1397–1408.

Liu, B., Qiu, X., Huang, Y., Hwang, K.C., Li, M., Liu, C., 2003. The size effect on void growth in ductile materials. J. Mech. Phys. Solids 51, 1171–1187.

Needleman, A., Rice, J.R., 1980. Plastic creep flow effects in the diffusive cavitation of grain boundaries. Acta Metal. 28 (10), 1315–1332.

Needleman, A., Tvergaard, V., Hutchinson, J.W., 1992. Void growth in plastic solids. In: Argon, A.S. (Ed.), Topics in Fracture and Fatigue. Springer-Verlag, pp. 145–178.

Needleman, A., Tvergaard, V., van der Giessen, E., 1995. Evolution of void shape and size in creeping solids. Int. J. Dam. Mech. 4 (2), 134–152.

Ponte Castañeda, P., Zaidman, M., 1994. Constitutive models for porous materials with evolving microstructure. J. Mech. Phys. Solids 42 (9), 1459–1497.

Ponte Castañeda, P., 1997. Nonlinear composite materials: effective constitutive behavior and microstructure evolution. In: Suquet, P. (Ed.), Continuum Micromechanics, CISM Courses and Lectures No. 377. Springer-Verlag, Vienna, pp. 131–195.

Rice, J.R., Chuang, T.-J., 1981. Energy variations in diffusive cavity growth. J. Am. Ceram. Soc. 64 (1), 46–53.

Sham, T.-L., Needleman, A., 1983. Effects of triaxial stressing on creep cavitation of grain boundaries. Acta Met. 31 (6), 919–926.

Subramanian, S.J., Sofronis, P., 2001. Modeling the interaction between densification mechanisms in powder compaction. Int. J. Solids Struct. 38 (44–45), 7899–7918.

Subramanian, S.J., 2001. Micromechanical modeling of the interaction of diffusion mechanisms and surface energy with nonlinear material deformation: applications to powder densification and void growth. Ph.D. Thesis, Department of Theoretical and Applied Mechanics, University of Illinois at Urbana-Champaign.

Subramanian, S.J., Sofronis, P., 2002. Calculation of a constitutive potential for isostatic powder compaction. Int. J. Mech. Sci. 44, 2239–2262.

Suo, Z., Wang, W., 1994. Diffusive void bifurcation in stressed solid. J. Appl. Phys. 76, 3410–3420.

Tvergaard, V., 1989. Material failure by void growth to coalescence. In: Hutchinson, J.W., Wu, T.Y. (Eds.), Advances in Applied Mechanics, vol. 27. pp. 83–151.

Wang, W., Suo, Z., 1997. Shape change of a pore in a stressed solid via surface diffusion motivated by surface and elastic energy variation. J. Mech. Phys. Solids 45, 709–729.